Langmuir

Article

pubs.acs.org/Langmuir

Solvent-Assisted Lipid Self-Assembly at Hydrophilic Surfaces: Factors Influencing the Formation of Supported Membranes

Seyed R. Tabaei,[†,‡] Joshua A. Jackman,[†,‡] Seong-Oh Kim,[†,‡] Vladimir P. Zhdanov,[†,‡,∥] and Nam-Joon Cho*[,†,‡,§]

[†]School of Materials Science and Engineering, Nanyang Technological University, 50 Nanyang Avenue 639798, Singapore

[‡]Centre for Biomimetic Sensor Science, Nanyang Technological University, 50 Nanyang Drive 637553, Singapore

[§]School of Chemical and Biomedical Engineering, Nanyang Technological University, 62 Nanyang Drive 637459, Singapore

[∥]Boreskov Institute of Catalysis, Russian Academy of Sciences, Novosibirsk 630090, Russia

Supporting Information

ABSTRACT: As a simple and efficient technique, the solvent-assisted lipid bilayer (SALB) formation method offers a versatile approach to fabricating a planar lipid bilayer on solid supports. Corresponding mechanistic aspects and the role of various governing parameters remain, however, to be better understood. Herein, we first scrutinized the effect of lipid concentration (0.01 to 5 mg/mL) and solvent type (isopropanol, *n*-propanol, or ethanol) on SALB formation on silicon oxide in order to identify optimal conditions for this process. The obtained fluid-phase lipid layers on silicon oxide were investigated by using the quartz crystal microbalance with dissipation monitoring, epifluorescence microscopy, and atomic force microscopy. The experimental results indicate that, in alcohol, lipid attachment to the substrate is reversible and reaches equilibrium in accordance with the bulk lipid concentration. During the solvent-exchange step, the water fraction increases and the deposited lipids are converted into planar bilayer fragments, along with the concurrent adsorption and rupture of micelles within an optimal lipid concentration range. In addition, fluid-phase lipid bilayers were successfully formed on other substrates (e.g., chrome, indium tin oxide, and titanium oxide) that are largely intractable to conventional methods (e.g., vesicle fusion). Moreover, gel-phase lipid bilayers were fabricated as well. Depending on the phase state of the lipid bilayer during fabrication, the corresponding adlayer mass varied by approximately 20% between the fluid- and gel-phase states in a manner which is consistent with the molecular packing of lipids in the two arrangements. Taken together, our findings help to explain the mechanistic details of SALB formation, optimize the corresponding procedure, and demonstrate the general utility for fabricating gel- and fluid-phase planar lipid bilayers.

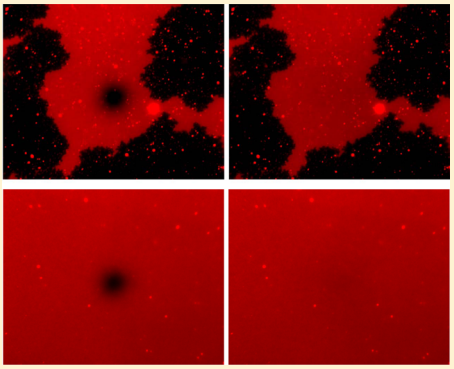

INTRODUCTION

Phospholipid assemblies on solid supports represent a useful class of model systems for studying membrane biology with surface-sensitive measurement tools.[1,2] The two-dimensional planar lipid bilayer is particularly attractive because it has a well-defined morphology similar to that in cells[3] and electrical insulating properties suitable for biosensor applications.[4] There are several different methods for forming planar bilayers on solid supports, including the Langmuir−Blodgett/Schaffer procedure, vesicle fusion, and bubble collapse deposition (reviewed in ref 5). Because of its high efficiency, vesicle fusion based on vesicle adsorption and rupture is the most widely used method. However, vesicle rupture occurs on only a subset of materials, mainly silica-based materials,[6,7] and is also limited to fluid-phase lipid compositions (gel-phase lipid vesicles have larger membrane bending rigidities[8] which hinder rupture). These factors restrict the general utility of vesicle fusion in forming planar bilayers.

From the perspective of the use of diverse substrate materials, a key shortcoming of vesicle fusion is that the adhesion energy required for vesicle rupture is typically much greater than that necessary to stabilize a planar bilayer on a solid support.[9] As a result, vesicles can adsorb but generally remain intact on substrates such as gold,[10] titanium oxide,[11] and aluminum oxide.[12] Depending on the case, the corresponding systems in general and the adhesion energy in particular can be influenced to promote vesicle rupture by changing vesicle properties (size,[11] lipid composition,[13] lamellarity,[14] and osmotic pressure[15]) and experimental conditions (ionic strength,[16] solution pH,[17] and temperature[18]). Alternatively, an amphipathic α-helical peptide can destabilize adsorbed vesicles and promote bilayer formation (e.g., on gold and titanium oxide).[19,20] In the aforementioned studies, good-

Received: January 25, 2014
Revised: February 5, 2015
Published: February 13, 2015

DOI: 10.1021/la5048497
Langmuir 2015, 31, 3125−3134

quality vesicle preparation[21] is a necessary and critical step before bilayer formation, and there has been interest in developing simpler bottom-up fabrication methods that do not require vesicle adsorption and rupture and can be extended to additional material surfaces.

One approach has focused on how solvent influences the self-assembly behavior of phospholipids.[22] In liquid solvents, the self-assembly varies depending on the physicochemical properties of the solute and solvent, and changes in solvent properties can induce lyotropic phase transitions in lipid aggregates.[23] Using small-angle X-ray scattering, Hohner et al.[24] determined that DMPC, DMTAP, and DMTAP/DMPC lipids dissolved (25 mg/mL) in isopropanol/water mixtures exhibit various phases with increasing fractions of water. At room temperature, for example, DMPC lipids in solution coexist in the form of monomers and inverted cylindrical micelles at water content below 24%. Monomers are observed in mixtures with water content of between 24 and 64%. With further increases in the water fraction, there is a coexistence of monomers and conventional elliptical micelles or spherical vesicles. If lipids are dissolved in isopropanol and the water fraction is gradually increased via titration up to an appreciable value, then the formation of a planar bilayer on a silicon oxide surface is observed.[24]

Inspired by solvent-assisted lipid self-assembly, a solvent-exchange protocol was developed whereby lipid in a pure organic solvent (isopropanol, ethanol, or *n*-propanol) is incubated with a solid support and then aqueous buffer solution is introduced to induce a series of phase transitions eventually yielding lamellar-phase lipid bilayers.[25] Using this solvent-assisted lipid bilayer (SALB) formation method, complete and homogeneous planar lipid bilayers were formed on silicon oxide and gold, the latter of which is intractable to conventional vesicle fusion. Importantly, bilayers formed by this method have mass and fluidic properties comparable to those of bilayers formed by the vesicle fusion method on equivalent substrates.[24,25] The influence of the solvent-exchange rate was also explored in order to understand how this factor influences the bilayer quality. In both of these studies[24,25] and a related one[26] (the subject of the latter study is the electrical properties of supported membranes), the focus has always been on the fabrication of a planar bilayer, and the corresponding measurement analysis followed traditional paradigms of planar lipid bilayers, i.e., comparison with benchmark cases of bilayers obtained via vesicle fusion.

With the practical application of the SALB formation method now established, it remains to be explored how, in more general terms, lipid self-assembly of this type proceeds at hydrophilic surfaces, starting with lipids deposited in alcohol. In previous work,[25] we investigated kinetic aspects related to the solvent-exchange step (i.e., flow conditions and lipid supply) and identified that a minimum lipid supply dictated by the balance of the bulk lipid concentration and solvent-exchange rate is required to ensure complete bilayer formation. The corresponding specifics of SALB formation remain to be investigated, including outlining the experimental requirements for successful bilayer formation. In the case of vesicle fusion, bilayer formation may occur via several channels[27] which were explicitly observed and studied in detail (e.g., ref 28.). A similar paradigm has not been established for the SALB formation method, and establishing such knowledge would be instructive in order to understand its mechanistic underpinning and scope of utility.

Here, we address this issue by scrutinizing the step of lipid adsorption in an organic solvent and the final properties of lipid layers formed by the SALB procedure. Attention is focused on the 1,2-dioleoyl-*sn*-glycero-3-phosphocholine (DOPC) lipid concentration and the type of organic solvent (isopropanol, *n*-propanol, or ethanol). Using quartz crystal microbalance with dissipation (QCM-D) monitoring, we measured those kinetics related to SALB experiments, including lipid adsorption in alcohol, and quantified the final adsorbed lipid layer formed after solvent exchange. Epifluorescence microscopy and atomic force microscopy (AFM) were also employed to investigate the structural properties of the lipid layers along with dynamic light scattering to characterize the properties of lipid aggregates in water/alcohol mixtures. The goal of these experiments was to optimize the SALB procedure, clarify the steps of SALB formation, and correlate deviations in measurement responses with the structural properties of the lipid layers.

Extending our learning, we further investigated the potential of the SALB method in forming planar lipid bilayers on other substrates (e.g., chrome, indium tin oxide, and titanium oxide) that are largely intractable to conventional methods (e.g., vesicle fusion). While previous work[25] has shown that a planar lipid bilayer can be formed on gold using this method, each substrate has different properties (some are known to prevent vesicle adsorption while others inhibit vesicle rupture), and verifying the general suitability of the approach is advantageous. Furthermore, additional QCM-D experiments were conducted using 1,2-dimyristoyl-*sn*-glycero-3-phosphocholine (DMPC) or 1,2-dipalmitoyl-*sn*-glycero-3-phosphocholine (DPPC) lipids above and below the gel-to-fluid phase-transition temperature of each lipid. In these experiments, the SALB procedure was executed with an aim toward forming gel- or fluid-phase lipid bilayers. Taken together, our findings help to explain the mechanistic details of SALB formation, optimize the corresponding procedure, and demonstrate its general utility for fabricating various lipid bilayer systems.

MATERIALS AND METHODS

Quartz Crystal Microbalance with Dissipation. A Q-Sense E4 instrument (Q-Sense AB, Gothenburg, Sweden) was employed in order to monitor changes in the resonance frequency (ΔF) and energy dissipation (ΔD) of a 5 MHz, AT-cut piezoelectric quartz crystal, as previously described.[29] The measurement data were collected at the n = 3−11 overtones, and the reported values were recorded at the third overtone ($\Delta F_{n=3}/3$). All QCM-D experiments were performed under flow-through conditions at a flow rate of 50 μL/min using a peristaltic pump (Ismatec Reglo Digital, Glattbrugg, Switzerland). With this flow rate and the measurement cell specifics (~100 μL flow channel with a 37 mm height, 35 mm width, and 63 mm depth section above the sensor crystal), the average flow velocity and time scale of solvent exchange in the chamber were approximately 0.12 mm/s and 1 min, respectively. The temperature of the flow cell was fixed at 24.00 ± 0.5 °C. For QCM-D experiments, all coated substrates were procured from Q-Sense AB (gold, QSX301; silicon oxide, QSX303; titanium oxide, QSX310; indium tin oxide, QSX999; aluminum oxide, QSX309). Before the experiment, the chips were rinsed with water and ethanol followed by drying with nitrogen air and treatment with oxygen plasma at the maximum radio frequency power for 1 min (Harrick Plasma, Ithaca, NY). For experiments reported below in Figures 6 and 7, 0.2 mg/mL bovine serum albumin (BSA) protein was added after forming lipid bilayer coatings in order to estimate the surface coverage of the lipid film, as compared to BSA adsorption on bare substrates.

Epifluorescence Microscopy. Fluorescence imaging experiments were performed using an inverted epifluorescence Eclipse TE 2000

DOI: 10.1021/la5048497
Langmuir 2015, 31, 3125−3134

microscope (Nikon, Tokyo, Japan) equipped with a 60× oil-immersion objective (NA 1.49) and an Andor iXon+ EMCCD camera (Andor Technology, Belfast, Northern Ireland). The acquired images consisted of 512 pixels × 512 pixels with a pixel size of 0.267 × 0.267 μm^2. For fluorescence microscopy experiments, 0.5 wt % rhodamine-modified 1,2-dihexadecanoyl-*sn*-glycero-3-phosphoethanolamine (rhodamine-DHPE) was included in the lipid mixture. The rhodamine-labeled DHPE-containing lipid samples were imaged using a TRITC filter set with a mercury lamp (Intensilight C-HGFIE, Nikon Corporation). For all fluorescence microscopy experiments, oxygen-plasma-treated glass coverslips (Menzel Gläser, Braunschweig, Germany) were used as the substrate.

Fluorescence Recovery after Photobleaching (FRAP) Measurements. Lateral lipid diffusion in lipid layers on silicon oxide was measured by the FRAP technique. After bilayer formation, a circular spot ($d \approx 20$ μm) was photobleached by a 532 nm, 100 mW laser beam. The bleaching time was ~5 s. The recovery was followed for 60 s by time-lapse recording with a 1 s interval. FRAP experimental data were analyzed using the Hankel transform method.[30]

Atomic Force Microscopy. An NX-Bio atomic force microscope (Park Systems, Suwon, South Korea), combined with an Eclipse Ti optical microscope (Nikon, Tokyo, Japan), was employed to image SALB experimental samples in contact mode. An ultrasharp silicon nitride BioLever minicantilever tip (Olympus, Tokyo, Japan) was used for all experiments. The tip has a tetrahedral shape, 110 kHz resonance frequency, and 0.09 N/m spring constant. Prior to experiment, the tip was treated with oxygen plasma (Harrick Plasma, Ithaca, New York, USA) for 5 min and sequentially rinsed with ethanol (70%), ultrapure water, and ethanol (70%) before finally drying with a gentle stream of nitrogen air. Experiments were conducted in an acoustic enclosure (Park Systems) with a temperature controller set at a constant temperature of 25 °C. AFM imaging was done on SALB samples immediately after the QCM-D experiment and postrinsing with aqueous buffer solution (10 mM Tris, 150 mM NaCl, pH 7.5).

RESULTS AND DISCUSSION

Stages of Bilayer Formation. A typical SALB experiment was performed as follows (Figure 1). First, aqueous buffer (10 mM Tris, 150 mM NaCl, pH 7.5) was injected into the QCM-D measurement chamber in order to establish the baseline for the frequency and energy dissipation signals. After 15 min of stabilization, the organic solution (i.e., isopropanol) was injected (arrow 1), which leads to a dramatic shift in the baseline within a short transient period. During this stage, the solution does not contain lipid and the observed large shift in the baseline is solely due to the density and viscosity difference between isopropanol and the aqueous buffer. After 15 min of additional stabilization, a freshly prepared isopropanol solution containing the desired concentration of DOPC lipid was injected (arrow 2), which led to a decrease in the frequency due to adsorption of lipid at the surface. No changes in the energy dissipation were observed during this stage. In the final stage (arrow 3), the lipid solution (isopropanol + lipid) was replaced by aqueous buffer solution (no lipid).

Using the SALB protocol at a fixed flow rate, we first identified the minimal lipid concentration required to form a planar bilayer on silicon oxide. Three concentrations of DOPC lipid in isopropanol solution were selected: 0.05, 0.1, and 0.25 mg/mL. For these concentrations, there were general trends in the changes in frequency (Figure 1A) and energy dissipation (Figure 1B). Concerning adsorbed lipids in isopropanol, we observed a linear dependence, $a + bc$ (a and b are constants), of the lipid-induced frequency shift on lipid concentration, c, in solution (Figure 1C). This shift is expected to be approximately proportional to the amount of adsorbed lipid. Furthermore, after the aqueous buffer replaced the isopropanol, the final

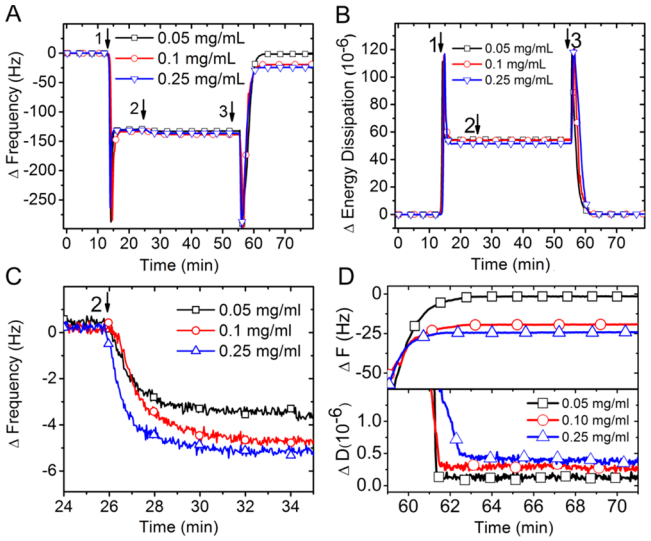

Figure 1. Minimum lipid concentration required for planar bilayer formation by the SALB method. Changes in QCM-D (A) frequency and (B) energy dissipation as functions of time are presented throughout the entire process. The measurement baseline was recorded in aqueous buffer solution, followed by solvent exchange with isopropanol (arrow 1), the addition of lipid in isopropanol solution at varying lipid concentrations (arrow 2), and solvent exchange with aqueous buffer solution (arrow 3). Panel (C) shows in detail the frequency shift after the moment indicated by arrow 2. Panel (D) depicts the final frequency (top) and energy dissipation shifts (bottom) after the completion of the SALB procedure.

changes in the QCM-D measurement signals varied appreciably depending on the lipid concentration (Figure 1D). At 0.05 mg/mL lipid, bilayer formation was not successful, as indicated by final changes in frequency and energy dissipation of −3 Hz and 0.07 × 10^{-6}, respectively. On the basis of the Sauerbrey relationship between the change in frequency and adsorbed mass, the final mass of adsorbed lipids corresponds to 12% of the mass, which is required to form a complete bilayer. At 0.1 mg/mL lipid, the final changes in frequency and energy dissipation were −19.2 Hz and 0.3 × 10^{-6}, respectively, which corresponds to a bilayer that is approximately 75% complete by mass. By contrast, at 0.25 mg/mL lipid, the final changes in frequency and energy dissipation were −25 Hz and 0.2 × 10^{-6}, respectively. These values are consistent with complete bilayers formed by the SALB procedure at a 2-fold-higher lipid concentration as well as by the conventional vesicle fusion method.[10]

Epifluorescence microscopy was employed in order to characterize the lipid structures in aqueous buffer solution after completion of the SALB procedure on glass (Figure 2). With increasing lipid concentration used in the SALB procedure, the fluorescence intensity of the lipid structures was more homogeneous. At 0.05 mg/mL lipid concentration, isolated lipid structures observed as diffraction-limited spots were distributed across the substrate and no fluid bilayer regions were observed (Figure 2A). At 0.1 mg/mL lipid concentration, there were microscopic lipid patches that did not span the entire field of view (100 μm × 100 μm) (Figure 2B). Fluorescence recovery after photobleaching (FRAP) measurements showed that the patches are fluidic, with a diffusion coefficient of 2.5 μm^2/s that is within the expected range for a fluid, planar bilayer[31] (Figure S1). As with lipid layers formed at 0.05 mg/mL lipid concentration, there were also smaller lipid

DOI: 10.1021/la5048497
Langmuir 2015, 31, 3125−3134

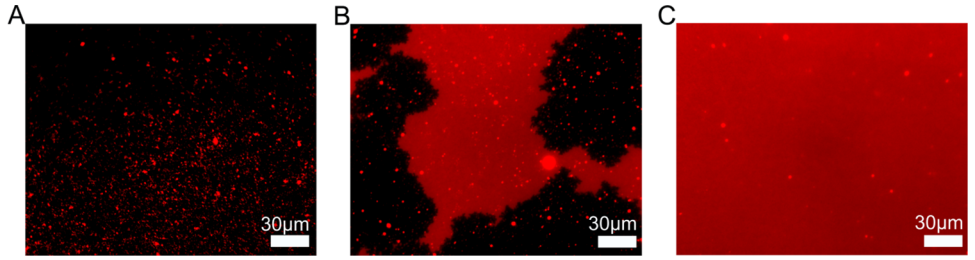

Figure 2. Threshold of lipid concentration for complete SALB formation. Epifluorescence microscopy was performed to characterize lipid layers on silicon oxide which were formed by the SALB procedure. Depending on the lipid concentration in isopropanol solution, the lipid structures observed on the substrate varied as follows: (A) isolated lipid spots at 0.05 mg/mL lipid concentration; (B) isolated lipid spots and microscopic lipid patches at 0.1 mg/mL lipid concentration; and (C) a homogeneous lipid layer at 0.25 mg/mL lipid concentration. Note that the image contrast is based on the normalized fluorescence intensity per image. The absolute mean fluorescence intensities of small spots in panels (A) and (B) are 420 ± 27 and 1355 ± 600 au, respectively.

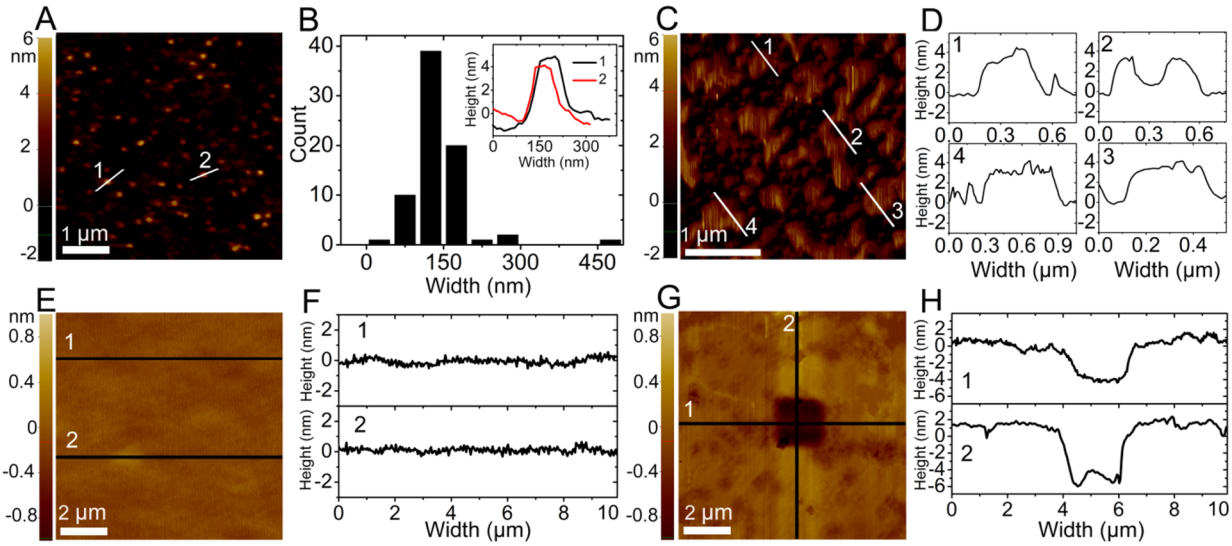

Figure 3. SALB lipid layers observed by atomic force microscopy. Imaging was performed to characterize the morphology of SALB-formed lipid layers on silicon oxide. The measurements were recorded in aqueous buffer solution following completion of the SALB procedure starting with various concentrations of lipid in isopropanol solution. For 0.05 mg/mL lipid concentration, (A) nanometer-scale lipid bilayer islands were observed and (B) corresponding histogram analysis showed that the average diameter was 133 ± 35 nm with a height of around 4 to 5 nm (see inset). For 0.1 mg/mL lipid concentration, (C) mesoscopic lipid bilayer fragments of nonuniform shape were observed and (D) corresponding histogram analysis showed that the height was around 4 to 5 nm. For 0.25 mg/mL lipid concentration, (E, F) the formation of a complete planar lipid bilayer was observed, as indicated by a smooth surface. (G) A 2 × 2 μm^2 segment of the lipid layer was removed via AFM tip scanning and (H) corresponding height profile analysis immediately after removal is presented.

structures visible as diffraction-limited spots on the substrate. To compare the isolated lipid structures in these two cases, we evaluated the total fluorescence intensity per isolated spot and determined that the spots formed at the higher lipid concentration had a 3-fold-greater mean fluorescence intensity per pixel than spots formed at the lower lipid concentration. The differences in fluorescence intensity could be due to either greater surface area or another membrane configuration (e.g., planar lipid bilayer vs vesicles) and is discussed further below. At 0.25 mg/mL lipid concentration, a homogeneous lipid structure was formed, with a diffusion coefficient of 2.5 $\mu m^2/s$ (Figures 2C and S2). In this case, small spots are also visible, but their coverage is appreciably lower than those in panels (A) and (B). Collectively, the trends in surface patches observed by epifluorescence microscopy are consistent with those in the QCM-D measurements and led us to scrutinize the morphology of the lipid layers by atomic force microscopy (AFM).

We next employed the AFM technique in order to characterize the morphology of lipid structures formed by the SALB procedure. To prepare samples for AFM imaging, SALB experiments on silicon oxide were conducted with QCM-D monitoring, and then the substrate was transferred to the AFM measurement chamber. This approach allowed us to establish a correlation between the QCM-D and AFM experimental results. For 0.05 mg/mL lipid, there was a final change in frequency of −2 Hz, and AFM height profile analysis identified isolated lipid structures of approximately 133 ± 35 nm diameter and a height of around 4 to 5 nm (Figure 3A,B). For 0.1 mg/mL lipid, mesoscopic lipid bilayer fragments of nonuniform shape were observed with similar height characteristics (Figure 3C,D). The size ranges of the isolated lipid structures formed at 0.05 and 0.1 mg/mL lipid concentrations, respectively, support that the difference in the absolute mean fluorescence intensity of diffraction-limited spots in each case is primarily due to the variation in the surface area of planar bilayer fragments. For the 0.25 mg/mL lipid, a complete planar bilayer was formed on the

DOI: 10.1021/la5048497
Langmuir 2015, 31, 3125−3134

basis of the appearance of a smooth homogeneous surface (Figure 3E,F). To confirm the formation of a planar bilayer, a 2 × 2 μm^2 segment of the lipid layer was removed by AFM tip scanning, and the corresponding height changes indicated that the lipid structure has a thickness of around 4 to 5 nm (Figure 3G,H). According to previous X-ray diffraction studies,[32] the DOPC lipid bilayer thickness is approximately 3.6 nm. Considering that an ∼1-nm-thick hydration layer stabilizes a planar bilayer on silicon oxide,[33] the thickness measured here is consistent with planar bilayer structures.

Dependence on Lipid Concentration. The effect of lipid concentration on the final outcome of the SALB experiments was also investigated over a wider lipid concentration range of up to 5 mg/mL and in different organic solvents (isopropanol, ethanol, and *n*-propanol). The corresponding adsorption kinetics of lipids in isopropanol are shown in the Supporting Information (Figure S3; for the other solvents, the results are similar). Within the tested lipid concentration range (between 0.05 and 5 mg/mL), lipid adsorption in alcohol rapidly reached steady state, and there was a linear relationship, $a + bc$ (Figures 1C and S4), between the amount of attached lipid and the bulk lipid concentration. The observation of steady state indicates either saturation of the adlayer or equilibrium (as previously proposed[24]) between the solution and adlayer. To distinguish between these two options, we performed an additional experiment. After the deposition of lipids in alcohol onto the substrate, a washing step with pure alcohol (without lipid) was performed and almost the entire adsorbed lipid mass was observed to be removed from the substrate. This finding indicates that there is equilibrium between lipids in solution and those attached to the substrate. Furthermore, the magnitude of the frequency shifts associated with the uptake varied depending on the type of organic solvent. The results were generally similar for isopropanol and *n*-propanol (e.g., −12 Hz at 5 mg/mL DOPC) and considerably smaller for ethanol (e.g., −6 Hz at 5 mg/mL DOPC). In other words, these findings show that the equilibrium depends on the type of organic solvent.

We recall that DOPC lipid adsorption (after the moment indicated by arrow 2 in Figure 2) occurs in nonaqeuous polar solvents. Levinger et al.[34] reported that DOPC lipids dissolved in nonpolar solvents (e.g., benzene) form inverted micelles, although the behavior of DOPC lipids in alcohols has not been studied to the best of our knowledge. While alcohols are not typically used as a medium for inverted micelle systems (nonpolar solvents are preferred[35]), anecdotal evidence[36−39] supports that DOPC lipids by analogy to lecithin compositions in general coexist as inverted micelles and monomers in alcohols. Earlier experiments[24] also indicate that DMPC lipids dissolved (25 mg/mL) in isopropanol/water mixtures coexist at low water content in the form of monomers and inverted cylindrical micelles. Furthermore, the lifetime of a discrete inverted micelle in solution is typically on the millisecond time scale due to micelle−micelle collisions and corresponding exchange processes that occur in a dynamic equilibrium,[40,41] so we assume that the attached species are predominately lipid monomers. Therefore, just before the replacement of the lipid solution by aqueous buffer solution (i.e., before arrow 3 in Figure 1), the surface appears to contain attached lipid monomers in an equilibrium that is dictated by the type of organic solvent. As explained above, even at high lipid concentrations in bulk solution (e.g., 5 mg/mL), the amount of attached lipid in this stage is no greater than half of the total amount required to form a complete planar bilayer. Accordingly, the solvent-exchange step plays a key role in facilitating the attachment of additional lipid mass to the substrate in addition to its influence on lipid self-assembly.

The interpretation of what happens during and after the replacement of the lipid solution by aqueous buffer solution is much more complex. One general observation here is that the time scale of the transition period in the observed kinetics is about 4 to 5 min (Figure 1A,B). This time is somewhat longer than the time scale of the solvent exchange in the chamber which is about 1 min, as described above in the Materials and Methods section. The latter time scale characterizes the solvent exchange on average. The solvent velocity near the surface is lower than the average one; accordingly, the time scale of the solvent exchange is expected to be a few times longer than 1 min. This means that in fact the observed kinetics occur during the replacement of the solution. Hence, with increasing water content of the solution, as already noted in the Introduction, lipids in solution undergo a series of phase transitions. Concurrently, albeit on a shorter time scale due to the kinetics of solvent exchange near the surface, the hydration of attached lipids would also occur and induce a series of phase transitions.

The QCM-D-measured characteristics of the lipid structures obtained at the end of the SALB procedure are presented in Figure 4. The reported values correspond to the final measurement after the completion of the SALB procedure, i.e., to the adsorbed lipids on silicon oxide in aqueous buffer solution. We defined bilayer formation based on final changes in frequency and energy dissipation between −25 and −30 Hz and less than 1 × 10^{-6}, respectively. On the basis of these

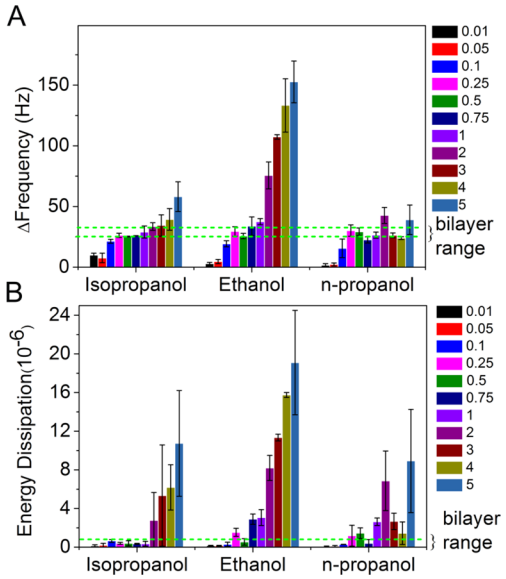

Figure 4. Influence of lipid concentration on planar bilayer formation by the SALB method. SALB experiments were performed using various organic solvents, including isopropanol, ethanol, and *n*-propanol, as a function of lipid concentration. QCM-D monitoring was employed to track solvent-assisted lipid self-assembly. The final measurement values (average and standard deviation from three independent experiments) are reported for changes in (A) frequency and (B) energy dissipation and correspond to adsorbed lipid layers in aqueous buffer solution following the completion of the SALB procedure. The dashed green lines correspond to the expected frequency and dissipation shifts for a complete planar bilayer (−30 Hz < ΔF < −25 Hz and ΔD < 1 × 10^{-6}).

DOI: 10.1021/la5048497
Langmuir 2015, 31, 3125−3134

criteria, the optimal lipid concentration range for forming planar bilayers was determined to be between 0.1 and 0.5 mg/mL and was largely independent of the type of organic solvent.

Interestingly, at higher lipid concentrations (in particular, 2 mg/mL or greater), there were significant deviations in the final measurement responses, as compared to typically expected values for planar bilayers.[42]

To interpret these deviations, the final change in QCM-D energy dissipation was plotted as a function of the corresponding frequency shift in Figure 5 (in which each data point corresponds to a specific lipid concentration). This diagram is divided into three qualitatively different regions corresponding to the formation of lipid bilayer islands up to a complete bilayer (region I) and more complex structures (regions II and III) discussed below. In isopropanol and *n*-propanol, high lipid concentrations led to the formation of lipid structures that had frequency shifts within the range of a planar bilayer (-25 ± 10 Hz) or below, albeit with large changes in energy dissipation of up to 12×10^{-6} (Figure 4 and region II in Figure 5, isopropanol and *n*-propanol). Deviations of this kind have not been previously observed for surface-adsorbed phospholipid assemblies in aqueous buffer solution and are inconsistent with the presence of unruptured vesicles, which is the main source of deviations reported in vesicle fusion experiments.

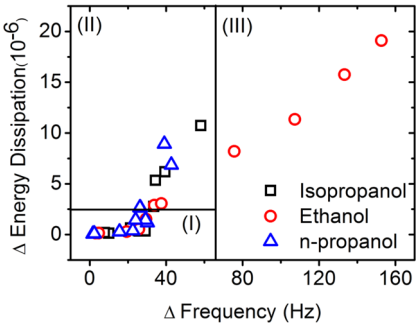

Figure 5. Change in QCM-D energy dissipation as a function of frequency shift at the end of SALB experiments. Each data point is replotted from Figure 4 and represents the average measurement from three independent experiments performed at a specific lipid concentration in a certain organic solvent including isopropanol (circles), *n*-propanol (triangles), and ethanol (squares).

To clarify this regime further, we employed fluorescence microscopy in order to investigate an SALB-formed lipid layer (from 5 mg/mL DOPC lipid in isopropanol) and observed a fluorescently homogeneous surface along with a low coverage of extended lipid structures protruding from the surface. The FRAP analysis indicated that the underlying lipid layer has a recovery profile that is consistent with a fluid planar bilayer (Figure S5). Similar behavior is also observed for SALB-formed lipid layers obtained from high lipid concentrations in *n*-propanol (Video S1 in Supporting Information). Previously, the addition of compounds such as fatty acids,[43] peptides,[44] and polymers[45] has been shown to induce the formation of extended lipid structures protruding from planar lipid bilayers. However, in all of these previous cases, the compounds were added to an already-formed planar bilayer, and the direct self-assembly of a lipid layer with such characteristics at a solid interface, to our knowledge, has not been reported. (Note that, in solution, lipid aggregates, e.g., wormlike normal micelles, may form upon addition of water to lecithins in organic solvent.[46]) Concerning the structural arrangement of lipids that leads to low-frequency and high-energy dissipation shifts, we may note that the weak attachment of extended filamentous virus phage particles to metal oxide surfaces shows a similar QCM-D measurement response[47] which suggests that lipid assemblies of this kind may also adopt an extended lipid structure. In such cases, a standing acoustic wave is established in the film and the film's viscoelastic component (i.e., extended lipids structures) would not result in an additional frequency shift.[48] Hence, in the present case, we conclude that, at high lipid concentration in isopropanol and *n*-propanol the SALB procedure induces the formation of a planar lipid bilayer along with a low coverage of extended lipid structures attached to the substrate.

By contrast, in ethanol, high lipid concentrations formed phospholipid assemblies with viscoelastic properties that appear to be more representative of intact vesicle layers than planar bilayers, based on large changes in frequency and dissipation greater than -80 Hz and 4×10^{-6}, respectively (Figure 4, ethanol; region III in Figure 5). To confirm the presence of lipid vesicles, we added 13 μM AH peptide, which is known[19] to rupture surface-adsorbed vesicles, to SALB-formed lipid layers (from 5 mg/mL lipid in ethanol) and observed vesicle rupture and the formation of a complete planar bilayer (Figure S6). Furthermore, in contrast to other organic solvents, FRAP analysis of lipid layers formed from high lipid concentrations in ethanol indicates that the layers have poor recovery and exhibit a granular appearance, both of which are consistent with intact vesicles (Video S2 in Supporting Information). As such, at high lipid concentration, there appears to be a relationship between the surface uptake (and corresponding phase behavior) of lipids in different organic solutions (i.e., isopropanol and *n*-propanol versus ethanol as described above) and the SALB procedure yielding lipid layers with specific characteristics. In light of the behavior of lipid aggregates in the water/alcohol mixtures, the data support that the phase transitions which occur during the solvent-exchange step depend on the organic solvent. Collectively, the findings indicate that a minimum lipid concentration (~0.1 mg/mL in our system; this value depends in part on the flow velocity) is required for complete bilayer formation and that above a certain concentration range this process may be accompanied by the self-assembly of additional extended lipid structures (in isopropanol and *n*-propanol) or appreciable vesicle adsorption (in ethanol). In isopropanol and *n*-propanol, at all lipid concentrations above the minimum threshold, bilayer formation occurs in addition to the formation of extended lipid structures. On the contrary, in ethanol, at high lipid concentrations, the FRAP analysis supports that there are adsorbed vesicles rather than a fluidic planar bilayer. It is also important to note that the details of these outcomes are based on our experimental procedure and depend on the specifics of the system under consideration.

With the guidelines above, we consider that in general the replacement of the organic solution with aqueous buffer solution results in the phase transition of attached lipids to form planar bilayer islands.[49,50] Concurrently, lipids in bulk solution also undergo phase transitions to form normal micelles and/or vesicles, some of which may attach to the surface depending on the rate of solvent exchange and lipid concentration. In our experiments, we observed mesoscopic islands (e.g., Figures 2A,B and 3) which, after their formation, do not change their shape on the time scale of the solvent replacement. This indicates that bilayer propagation occurs

DOI: 10.1021/la5048497
Langmuir 2015, 31, 3125−3134

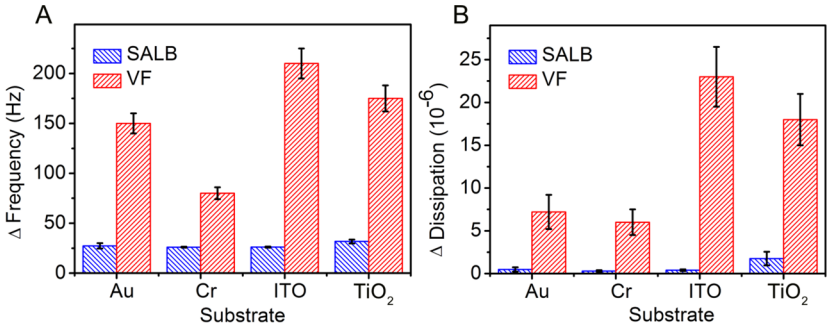

Figure 6. QCM-D final frequency and energy dissipation shifts on different material substrates. Vesicle fusion (VF) experiments were conducted using 72-nm-diameter DOPC lipid vesicles in aqueous buffer (10 mM Tris, 150 mM NaCl, pH 7.5). SALB experiments were performed with 0.5 mg/mL DOPC lipid in isopropanol, and the solvent-exchange solution was the same aqueous buffer.

primarily via rupture of newly arrived micelles or vesicles. (Note that the diffusion of vesicles on silicon oxide is slow.[51]) In light of bilayer formation on gold via the SALB procedure,[25] micelle attachment appears to be the predominant event in cases of bilayer formation although vesicle attachment may occur substantially under specific conditions and lead to deviations (e.g., high lipid concentration using ethanol).

Overall, the situation appears to be relatively simple at low lipid concentrations (e.g., 0.05 mg/mL). In this case, as already noted, the process seems to primarily include the formation of planar bilayer islands. One of the likely scenarios here is that with increasing lipid concentration the islands grow primarily via attachment and subsequent rupture of normal micelles as was discussed earlier.[25] At lipid concentrations of up to 0.5 mg/mL, the SALB experiments (Figures 1−4) resulted in the formation of mesoscopic lipid bilayer islands up to a complete lipid bilayer (region I in Figure 5). It is also of interest that, with the lipid concentration increasing above 0.5 mg/mL, the final QCM-D measurement values indicate that the adlayer may contain additional lipid structures. From a practical perspective, the experiments confirm that the SALB procedure can form planar bilayers above a minimum lipid concentration (under fixed flow conditions) and provide key information enabling its optimization and interpretation of measurement data obtained from the corresponding experiments. In light of the above finding that micelles, not vesicles, play an important role in the bilayer formation process, the SALB method has good potential for fabricating planar lipid bilayers on solid supports that do not support vesicle rupture. While bilayer formation on gold has already been demonstrated by the SALB procedure,[25] the range of substrates amenable to bilayer fabrication by this method remains to be investigated, with respect to both the material composition and lipid−substrate interaction.

Bilayer Formation on Different Substrates. We next investigated planar lipid bilayer formation by the SALB procedure on various substrates—chrome, titanium oxide, and indium tin oxide—that are intractable by the vesicle fusion method, as previously reported by Groves et al.[52] Reference measurements were also made on a gold substrate. To track the adsorption process and final mass and viscoelastic properties of the adlayers, QCM-D monitoring was employed (Figure 6). Vesicle adsorption measurements were first performed on the test substrates. On titanium oxide and indium tin oxide, significant vesicle uptake was observed with final changes in frequency and energy dissipation of around −150 to −200 Hz and 15 to 23 × 10^{-6}, respectively. These trends are similar to those for gold, although there is lower energy dissipation on gold which suggests a greater deformation of adsorbed vesicles. By contrast, on chrome, the final changes in frequency and energy dissipation were only −80 Hz and 6 × 10^{-6}, respectively. Hence, vesicle adsorption is energetically more favorable on chrome because the final values are consistent with even more appreciable deformation, albeit an insufficient amount to promote vesicle rupture.

SALB experiments were next performed on the same set of substrates, with a 0.5 mg/mL DOPC lipid concentration in isopropanol. For these experiments, the SALB procedure led to the formation of lipid films with final changes in frequency and energy dissipation of approximately −26 Hz and 0.5 × 10^{-6}, respectively, on indium tin oxide and chrome, which are in agreement with results obtained on gold. The nonspecific adsorption of BSA protein to bare and lipid-bilayer-coated substrates was also measured in order to estimate the surface coverage of the lipid film (Table S1). On indium tin oxide and chrome, the coverage was around 84 and 94%, respectively. Taken together, the surface coverage and mass density of the lipid films are consistent with the formation of single lipid bilayer coatings. Furthermore, on titanium oxide, the final changes in frequency and energy dissipation were approximately −30 Hz and 2 × 10^{-6}, respectively. The lipid−substrate interaction on titanium oxide is believed to be governed by a strong repulsive hydration force under nearly neutral pH conditions.[53] Accordingly, a thicker hydration layer than normally expected may be present in this case and may explain the higher shifts. In this case, the surface coverage of the lipid film was approximately 87%, again supporting the formation of a single lipid bilayer coating. Overall, these findings indicate that the lipid−substrate interaction plays an important role in influencing the properties of the lipid film formed by the SALB procedure. To verify this condition, an additional experiment was performed on silicon oxide, and the aqueous buffer solution used for solvent exchange had a pH value of 12. In such environments, an icelike hydration layer forms on silicon oxide which is resistant to vesicle adsorption.[17] After completion of the SALB procedure, the final changes in frequency and energy dissipation were approximately −11 Hz and 3.2 × 10^{-6}, respectively. Compared to results obtained under nearly neutral pH conditions, these values indicate that bilayer formation on silicon oxide was incomplete and likely inhibited by a repulsive lipid−substrate interaction. Therefore, the SALB procedure is appropriate for the fabrication of planar lipid bilayers on substrates under conditions which promote attractive lipid−substrate interactions, albeit with insufficient energetics for vesicle rupture.

DOI: 10.1021/la5048497
Langmuir 2015, 31, 3125−3134

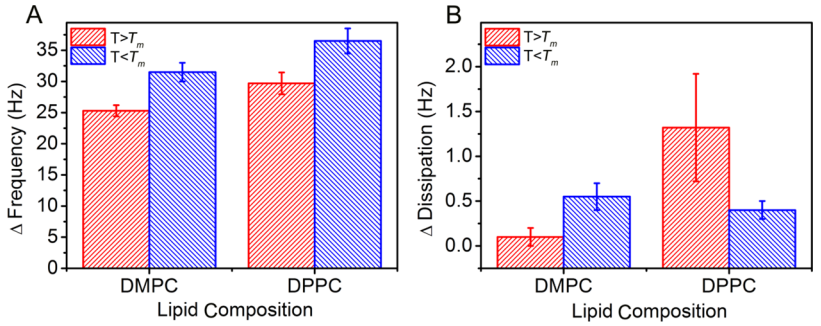

Figure 7. QCM-D final frequency and energy dissipation shifts for DMPC and DPPC lipids in different membrane phase states. SALB experiments were performed with 0.5 mg/mL lipid in isopropanol, and the solvent-exchange solution was the same aqueous buffer. For DMPC lipid, the experiments were performed at 20 °C (gel) and 35 °C (fluid), respectively. For DPPC lipid, the corresponding temperatures were 24 °C (gel) and 50 °C (fluid), respectively.

Influence of the Membrane Phase State. Another key issue of bilayer fabrication is the membrane phase (gel or fluid) state. Vesicle fusion requires a fluid-phase lipid composition which limits the range of possible lipid compositions or the experiments and the corresponding vesicle preparation step must be conducted at temperatures well above the highest phase-transition temperature (T_m) in the lipid mixture.[54] To investigate if the SALB procedure is suitable for both gel- and fluid-phase lipid compositions, QCM-D experiments were performed on silicon oxide with DMPC and DPPC lipids above and below the corresponding phase-transition temperature (T_m = 23 and 41 °C, respectively; Figure 7). All experimental stages were conducted at the same temperature in order to avoid temperature-dependent artifacts in the QCM-D data interpretation unless otherwise noted. For DMPC lipid, the final frequency shifts at 20 °C (gel) and 35 °C (fluid) were −31.5 ± 1.5 and −25.3 ± 0.9 Hz, respectively (Figure 7A). Likewise, the final energy dissipation shifts at the two temperatures were 0.5 ± 0.1 and (0.1 ± 0.1) × 10^{-6} Hz, respectively (Figures 7B and S7). The nonspecific adsorption of BSA protein to the lipid bilayers formed was negligible in both cases (<1 Hz). For rigid adlayers of this kind, the frequency shift is directly proportional to the adsorbate mass according to the Sauerbrey relationship,[55] and it can be inferred that the surface mass density of the gel-phase lipid bilayer is 24.5% greater than that of the fluid-phase lipid bilayer. The mass difference is consistent with the change in the molecular packing area per DMPC lipid which increases from 47.5 Å (gel) to 62 Å (fluid), a 31% increase.[56]

Similar experiments were also performed with the DPPC lipid composition. In this case, the final frequency shifts at 24 °C (gel) and 50 °C (fluid) were −36.5 ± 2.0 and −29.7 ± 1.8 Hz, respectively, and the final energy dissipation shifts at the two temperatures were 0.4 ± 0.1 and (1.3 ± 0.6) × 10^{-6}, respectively (Figures 7A,B and S8). BSA protein attachment to the lipid bilayers formed was again low in both cases (<2 Hz), indicating greater than 96% completion. On the basis of the Sauerbrey relationship, the surface mass density of the gel-phase lipid bilayer is 21% greater than that of the fluid-phase lipid bilayer. For the DPPC lipid, the molecular packing area per lipid increases 47.5 Å (gel) to 70 Å (fluid)—a 47% increase—and the trend is consistent.[56] For optimal results with gel-phase DPPC lipid compositions, the planar lipid bilayer (prepared below T_m) can be briefly heated to above the T_m and then cooled again. This step has a minimal effect on the frequency shift but can significantly decrease the energy dissipation signal, which suggests that some extended lipid structures may be removed during annealing. Annealing was not required for optimal bilayer formation with the DMPC lipid composition. Interestingly, the frequency shifts for DPPC lipid bilayers were approximately 15% greater than for DMPC lipid bilayers in the equivalent phase, and the trend is consistent with the difference in molecular mass of the two phospholipids. Taken together, the SALB method is a promising alternative to fabricating gel-phase lipid bilayers as compared to standard fabrication techniques.

CONCLUSIONS

Herein, we investigated mechanistic aspects of planar bilayer formation on silicon oxide by the SALB method. It was determined that the SALB procedure results in planar bilayer formation via micelle (or vesicle) rupture at the boundaries of bilayer islands. Accordingly, there was a minimum lipid concentration required for bilayer formation on silicon oxide as well as an optimal concentration range (0.1−0.5 mg/mL lipid). Below this concentration range, an incomplete bilayer formed. Above this concentration range, additional lipid structures may form, including those which appear to contain extended lipid aggregates or intact vesicles, depending on which organic solvent is used in the SALB procedure. The situation for bilayer formation on gold is similar. Physically, the effect of lipid concentration on the SALB formation process can be rationalized by taking into account that, in this case, during solvent exchange there is an interplay between the lipid supply to the substrate and lipid removal from the chamber. An increase in lipid concentration facilitates bilayer formation while an increase in the flow rate may suppress it. Qualitatively, these effects can be described by using a generic kinetic model that was proposed earlier.[25]

Mechanistically, our study shows that lipid attachment to silicon oxide takes place at low fractions of water in the solution in the situation in which dissolved lipid coexists in the form of monomers and inverted micelles. The corresponding lipid uptake is, however, relatively small. The subsequent solvent-exchange stage plays a key role in facilitating the attachment of additional lipid mass to the substrate and the formation of a lipid bilayer. The latter stage seems to occur via adsorption and rupture of conventional micelles (or vesicles). The final lipid uptake depends on the initial lipid concentration in solution as shown here and also on the flow rate as was shown in our previous study.[25] On the basis of these mechanistic factors, we further demonstrated that planar lipid bilayers can be formed

DOI: 10.1021/la5048497
Langmuir 2015, 31, 3125−3134

on various substrates, including chrome, indium tin oxide, and titanium oxide. Indeed, the SALB approach is particularly useful for fabricating bilayers on substrates which support vesicle adsorption but have insufficient energetics to promote vesicle rupture. In addition, the SALB method is able to form both gel- and fluid-phase planar lipid bilayers, and the trends in the QCM-D frequency shifts are consistent with the molecular packing of lipids in both membrane phase states. Taken together, all of the aforementioned findings clarify the mechanism of the SALB formation process and substantiate the method's general utility in fabricating planar bilayers on hydrophilic solid supports.

■ ASSOCIATED CONTENT

Supporting Information

Detailed information on FRAP analysis of lipid layers formed by the SALB method, lipid adsorption in isopropanol, QCM-D analysis of peptide-induced vesicle rupture, SALB experiments in different membrane phase states, and BSA protein attachment to multiple substrates. Videos S1−S2 are also provided and show FRAP analysis of lipid layers formed by the SALB procedure at high lipid concentration. This material is available free of charge via the Internet at http://pubs.acs.org.

■ AUTHOR INFORMATION

Corresponding Author

*E-mail: njcho@ntu.edu.sg.

Notes

The authors declare no competing financial interest.

■ ACKNOWLEDGMENTS

We acknowledge support from the National Research Foundation (NRF-NRFF2011-01), the National Medical Research Council (NMRC/CBRG/0005/2012), and Nanyang Technological University for N.-J.C. J.A.J. is a recipient of the Nanyang President's Graduate Scholarship. V.P.Z. is a recipient of the Tan Chin Tuan Exchange Fellowship at Nanyang Technological University.

■ REFERENCES

(1) Hardy, G. J.; Nayak, R.; Zauscher, S. Model cell membranes: techniques to form complex biomimetic supported lipid bilayers via vesicle fusion. *Curr. Opin. Colloid Interface Sci.* **2013**, *18*, 448−458.

(2) Mashaghi, A.; Mashaghi, S.; Reviakine, I.; Heeren, R. M.; Sandoghdar, V.; Bonn, M. Label-free characterization of biomembranes: from structure to dynamics. *Chem. Soc. Rev.* **2014**, *43*, 887−900.

(3) Castellana, E. T.; Cremer, P. S. Solid supported lipid bilayers: from biophysical studies to sensor design. *Surf. Sci. Rep.* **2006**, *61*, 429−444.

(4) Sackmann, E. Supported membranes: scientific and practical applications. *Science* **1996**, *271*, 43−48.

(5) Czolkos, I.; Jesorka, A.; Orwar, O. Molecular phospholipid films on solid supports. *Soft Matter* **2011**, *7*, 4562−4576.

(6) Richter, R. P.; Bérat, R.; Brisson, A. R. Formation of solid-supported lipid bilayers: an integrated view. *Langmuir* **2006**, *22*, 3497−3505.

(7) Reimhult, E.; Kumar, K. Membrane biosensor platforms using nano-and microporous supports. *Trends Biotechnol.* **2008**, *26*, 82−89.

(8) Vitkova, V.; Petrov, A. Lipid bilayers and membranes: material properties. *Adv. Planar Lipid Bilayers Liposomes* **2013**, *17*, 89−138.

(9) Tero, R.; Ujihara, T.; Urisu, T. Lipid bilayer membrane with atomic step structure: supported bilayer on a step-and-terrace TiO2 (100) surface. *Langmuir* **2008**, *24*, 11567−11576.

(10) Keller, C.; Kasemo, B. Surface specific kinetics of lipid vesicle adsorption measured with a quartz crystal microbalance. *Biophys. J.* **1998**, *75*, 1397−1402.

(11) Reimhult, E.; Hook, F.; Kasemo, B. Vesicle adsorption on SiO_2 and TiO_2: dependence on vesicle size. *J. Chem. Phys.* **2002**, *117*, 7401−7404.

(12) Mager, M. D.; Almquist, B.; Melosh, N. A. Formation and characterization of fluid lipid bilayers on alumina. *Langmuir* **2008**, *24*, 12734−12737.

(13) Richter, R.; Mukhopadhyay, A.; Brisson, A. Pathways of lipid vesicle deposition on solid surfaces: a combined QCM-D and AFM study. *Biophys. J.* **2003**, *85*, 3035−3047.

(14) Jackman, J. A.; Zhao, Z.; Zhdanov, V. P.; Frank, C. W.; Cho, N.-J. Vesicle adhesion and rupture on silicon oxide: influence of freeze−thaw pretreatment. *Langmuir* **2014**, *30*, 2152−2160.

(15) Reimhult, E.; Höök, F.; Kasemo, B. Intact vesicle adsorption and supported biomembrane formation from vesicles in solution: influence of surface chemistry, vesicle size, temperature, and osmotic pressure. *Langmuir* **2003**, *19*, 1681−1691.

(16) Boudard, S.; Seantier, B.; Breffa, C.; Decher, G.; Felix, O. Controlling the pathway of formation of supported lipid bilayers of DMPC by varying the sodium chloride concentration. *Thin Solid Films* **2006**, *495*, 246−251.

(17) Cremer, P. S.; Boxer, S. G. Formation and spreading of lipid bilayers on planar glass supports. *J. Phys. Chem. B* **1999**, *103*, 2554−2559.

(18) Reimhult, E.; Höök, F.; Kasemo, B. Temperature dependence of formation of a supported phospholipid bilayer from vesicles on SiO_2. *Phys. Rev. E* **2002**, *66*, 051905.

(19) Cho, N. J.; Cho, S. J.; Cheong, K. H.; Glenn, J. S.; Frank, C. W. Employing an amphipathic viral peptide to create a lipid bilayer on Au and TiO_2. *J. Am. Chem. Soc.* **2007**, *129*, 10050−1.

(20) Goh, H. Z.; Jackman, J. A.; Cho, N.-J. AH peptide-mediated formation of charged planar lipid bilayers. *J. Phys. Chem. B* **2014**, *118*, 3616−3621.

(21) Cho, N.-J.; Frank, C. W.; Kasemo, B.; Höök, F. Quartz crystal microbalance with dissipation monitoring of supported lipid bilayers on various substrates. *Nat. Protoc.* **2010**, *5*, 1096−1106.

(22) Szoka, F.; Papahadjopoulos, D. Procedure for preparation of liposomes with large internal aqueous space and high capture by reverse-phase evaporation. *Proc. Natl. Acad. Sci. U.S.A.* **1978**, *75*, 4194−4198.

(23) Seddon, J.; Templer, R. Polymorphism of lipid-water systems. *Handb. Biol. Phys.* **1995**, *1*, 97−160.

(24) Hohner, A.; David, M.; Rädler, J. Controlled solvent-exchange deposition of phospholipid membranes onto solid surfaces. *Biointerphases* **2010**, *5*, 1−8.

(25) Tabaei, S. R.; Choi, J. H.; Goh, H. Z.; Zhdanov, V. P.; Cho, N.-J. Solvent-assisted lipid bilayer formation on silicon dioxide and gold. *Langmuir* **2014**, *30*, 10363−10373.

(26) Wiegand, G.; Arribas-Layton, N.; Hillebrandt, H.; Sackmann, E.; Wagner, P. Electrical properties of supported lipid bilayer membranes. *J. Phys. Chem. B* **2002**, *106*, 4245−4254.

(27) Keller, C.; Glasmästar, K.; Zhdanov, V.; Kasemo, B. Formation of supported membranes from vesicles. *Phys. Rev. Lett.* **2000**, *84*, 5443.

(28) Andrecka, J.; Spillane, K. M.; Ortega-Arroyo, J.; Kukura, P. Direct observation and control of supported lipid bilayer formation with interferometric scattering microscopy. *ACS Nano* **2013**, *7*, 10662−10670.

(29) Rodahl, M.; Hook, F.; Krozer, A.; Brzezinski, P.; Kasemo, B. Quartz crystal microbalance setup for frequency and Q-factor measurements in gaseous and liquid environments. *Rev. Sci. Instrum.* **1995**, *66*, 3924−3930.

(30) Jönsson, P.; Jonsson, M. P.; Tegenfeldt, J. O.; Höök, F. A method improving the accuracy of fluorescence recovery after photobleaching analysis. *Biophys. J.* **2008**, *95*, 5334−5348.

(31) Przybylo, M.; Sýkora, J.; Humpolíčková, J.; Benda, A.; Zan, A.; Hof, M. Lipid diffusion in giant unilamellar vesicles is more than 2

DOI: 10.1021/la5048497
Langmuir 2015, 31, 3125−3134

times faster than in supported phospholipid bilayers under identical conditions. *Langmuir* **2006**, *22*, 9096−9099.
(32) Gandhavadi, M.; Allende, D.; Vidal, A.; Simon, S.; McIntosh, T. Structure, composition, and peptide binding properties of detergent soluble bilayers and detergent resistant rafts. *Biophys. J.* **2002**, *82*, 1469−1482.
(33) Boxer, S. G. Molecular transport and organization in supported lipid membranes. *Curr. Opin. Chem. Biol.* **2000**, *4*, 704−709.
(34) Levinger, N. E.; Costard, R.; Nibbering, E. T.; Elsaesser, T. Ultrafast energy migration pathways in self-assembled phospholipids interacting with confined water. *J. Phys. Chem. A* **2011**, *115*, 11952−11959.
(35) Correa, N. M.; Silber, J. J.; Riter, R. E.; Levinger, N. E. Nonaqueous polar solvents in reverse micelle systems. *Chem. Rev.* **2012**, *112*, 4569−4602.
(36) Elworthy, P.; McIntosh, D. The effect of solvent dielectric constant on micellisation by lecithin. *Kolloid-Z. Z. Polym., Suppl.* **1964**, *195*, 27−34.
(37) Aarts, P.; Gijzeman, O.; Kremer, J.; Wiersema, P. Dynamics of phospholipid aggregation in ethanol-water solutions. *Chem. Phys. Lipids* **1977**, *19*, 267−274.
(38) Tinker, D. O.; Saunders, L. Studies of isotropic phosphatidyl choline-n-propanol-water systems. *Chem. Phys. Lipids* **1968**, *2*, 316−329.
(39) Klose, G. Phosphorus-31 studies on lecithin in ethanol solutions. *Chem. Phys. Lipids* **1975**, *15*, 9−14.
(40) Fletcher, P. D.; Howe, A. M.; Robinson, B. H. The kinetics of solubilisate exchange between water droplets of a water-in-oil microemulsion. *J. Chem. Soc., Faraday Trans. 1* **1987**, *83*, 985−1006.
(41) Luisi, P.; Giomini, M.; Pileni, M. a.; Robinson, B. Reverse micelles as hosts for proteins and small molecules. *Biochim. Biophys. Acta, Rev. Biomembr.* **1988**, *947*, 209−246.
(42) Hamai, C.; Yang, T.; Kataoka, S.; Cremer, P. S.; Musser, S. M. Effect of average phospholipid curvature on supported bilayer formation on glass by vesicle fusion. *Biophys. J.* **2006**, *90*, 1241−1248.
(43) Thid, D.; Benkoski, J. J.; Svedhem, S.; Kasemo, B.; Gold, J. DHA-induced changes of supported lipid membrane morphology. *Langmuir* **2007**, *23*, 5878−5881.
(44) Domanov, Y. A.; Kinnunen, P. K. Antimicrobial peptides temporins B and L induce formation of tubular lipid protrusions from supported phospholipid bilayers. *Biophys. J.* **2006**, *91*, 4427−4439.
(45) Rossetti, F. F.; Reviakine, I.; Csúcs, G.; Assi, F.; Vörös, J.; Textor, M. Interaction of poly(L-lysine)-g-poly(ethylene glycol) with supported phospholipid bilayers. *Biophys. J.* **2004**, *87*, 1711−1721.
(46) Palazzo, G. Wormlike reverse micelles. *Soft Matter* **2013**, *9*, 10668−10677.
(47) Chen, H.; Su, X.; Neoh, K.-G.; Choe, W.-S. QCM-D analysis of binding mechanism of phage particles displaying a constrained heptapeptide with specific affinity to SiO_2 and TiO_2. *Anal. Chem.* **2006**, *78*, 4872−4879.
(48) Granéli, A.; Edvardsson, M.; Höök, F. DNA-based formation of a supported, three-dimensional lipid vesicle matrix probed by QCM-D and SPR. *ChemPhysChem* **2004**, *5*, 729−733.
(49) Perkin, S.; Kampf, N.; Klein, J. Stability of self-assembled hydrophobic surfactant layers in water. *J. Phys. Chem. B* **2005**, *109*, 3832−3837.
(50) Macakova, L.; Blomberg, E.; Claesson, P. M. Effect of adsorbed layer surface roughness on the QCM-D response: focus on trapped water. *Langmuir* **2007**, *23*, 12436−12444.
(51) Klacar, S.; Dimitrievski, K.; Kasemo, B. Influence of surface pinning points on diffusion of adsorbed lipid vesicles. *J. Phys. Chem. B* **2009**, *113*, 5681−5685.
(52) Groves, J. T.; Ulman, N.; Cremer, P. S.; Boxer, S. G. Substrate-membrane interactions: mechanisms for imposing patterns on a fluid bilayer membrane. *Langmuir* **1998**, *14*, 3347−3350.
(53) Jackman, J. A.; Zan, G. H.; Zhao, Z.; Cho, N.-J. Contribution of the Hydration Force to Vesicle Adhesion on Titanium Oxide. *Langmuir* **2014**, *30*, 5368−5372.
(54) Nayar, R.; Hope, M. J.; Cullis, P. R. Generation of large unilamellar vesicles from long-chain saturated phosphatidylcholines by extrusion technique. *Biochim. Biophys. Acta, Biomembr.* **1989**, *986*, 200−206.
(55) Sauerbrey, G. Verwendung von Schwingquarzen zur Wägung dünner Schichten und zur Mikrowägung. *Z. Phys.* **1959**, *155*, 206−222.
(56) Lichtenberg, D.; Schmidt, C. Molecular packing and stability in the gel phase of curved phosphatidylcholine vesicles. *Lipids* **1981**, *16*, 555−557.

DOI: 10.1021/la5048497
Langmuir 2015, 31, 3125−3134